International Journal of Thermophysics, Vol. 16, No. 5, 1995

Simultaneous Measurement of Surface Tension and Kinematic Viscosity Using Thermal Fluctuations[1]

T. Nishio[2] and Y. Nagasaka[2,3]

We have developed a surface laser-light scattering apparatus to measure simultaneously surface tension and kinematic viscosity. In this method, we can obtain the surface properties by the laser heterodyne detection of light scattered from thermally excited capillary waves (called "ripplon"), which are typically of low amplitude (~ 1 nm) and a characteristic wavelength ($\sim 100\,\mu$m). Two gratings ($d = 100$ and $200\,\mu$m) were employed to select the wave number of the capillary waves and to produce a reference beam for heterodyne detection. It was found through an experimental study on water that this contact-free method has considerable potential for application to measurements under extreme conditions such as high temperatures and high pressures.

KEY WORDS: kinematic viscosity; ripplon; surface laser-light scattering method; surface tension.

1. INTRODUCTION

In the field of semiconductor production, it is required to control and simulate the convection in the melts to obtain higher-quality single crystals [1]. Although the thermophysical properties of semiconductor melts such as molten Si, GaAs, and InP are needed, there have been a very limited number of experimental studies, with differences often far beyond their claimed accuracies. This is because the thermophysical properties measurements of molten semiconductors are extremely difficult owing to their high melting temperatures and corrosiveness. In many cases, the conventional techniques may not be suitable for the measurement.

[1] Paper presented at the Twelfth Symposium on Thermophysical Properties, June 19–24, 1994, Boulder, Colorado, U.S.A.

[2] Department of Mechanical Engineering, Keio University, 3-14-1, Hiyoshi, Yokohama 223, Japan.

[3] To whom correspondence should be addressed.

0195-928X/95/0900-1087$07.50/0

As a potential technique to answer the above-mentioned requirements, we have been developing the surface laser-light scattering (SLLS) method to measure the surface tension and kinematic viscosity of liquids [2, 3]. The characteristics of the SLLS method are as follows. (i) The surface tension and kinematic viscosity can be determined simply by detecting the scattered laser light from a liquid surface at thermal and mechanical equilibrium, therefore this method has an advantage when it is difficult to insert an actuator in a sample such as high-temperature corrosive melts. (ii) Since measurement can be performed successively and rapidly, it is, in principle, possible to detect the temporal behavior of the surface properties. The first SLLS experiment was started by Katyl and Ingard [4, 5]. Subsequently, there are some examples of studies on the measurements of viscoelastic monomolecular films [6] and the application to crude oil [7, 8]. The final goal of the present study is to measure the surface tension and the kinematic viscosity of molten Si at high temperatures. As the first step, in the present paper, a new apparatus to measure the surface tension and kinematic viscosity simultaneously by the SLLS method will be described.

2. PRINCIPLE OF MEASUREMENT

Liquid surfaces are constantly being deformed by the thermal fluctuations in the form of waves. These waves can be represented as a spatial Fourier series of thermally excited capillary waves which are typically of low amplitude (~ 1 nm) and with a characteristic wavelength ($\sim 100\,\mu$m) [5]. The temporal behavior of these thermally generated waves (called "ripplon") is governed by the thermophysical properties of the liquid, principally surface tension and viscosity. Since each ripplon acts like a moving diffraction grating, a laser beam incident on the surface experiences a small frequency shift due to Doppler effect (Brillouin scattering) (Fig. 1a). By detecting these frequency shifts using the laser heterodyne technique, it is possible to measure simultaneously the surface tension and kinematic viscosity.

2.1. Dispersion Relation

The behavior of these thermally driven capillary waves can be described by using classical hydrodynamics since they have microscopic amplitude but macroscopic wavelength. Hence, the wavelengths of these capillary waves are short enough that the effect of gravity can be neglected, their action depends only on the surface tension for restoration, and on kinematic viscosity for damping. Defining the $z=0$ plane as the liquid surface and

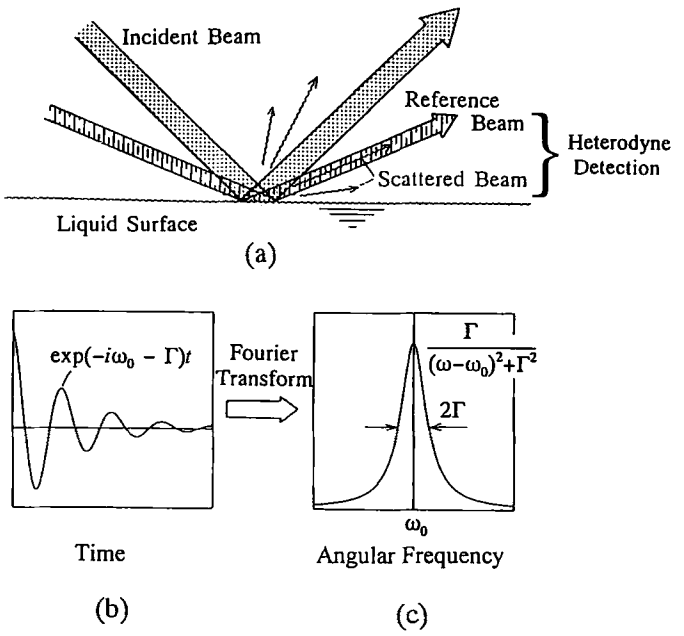

Fig. 1. (a) Schematic diagram of the reference and scattered beams used in the heterodyne detection technique. (b) Schematic diagram of the temporal decay of the surface wave. (c) Fourier transform to line shape of the decay surface wave.

waves of a ripplon propagating in the x direction only, the displacement ζ of the surface can be expressed as

$$\zeta(x, t) = \zeta_0 \cos(kx) \exp(\alpha t) \tag{1}$$

where ζ_0 is the initial amplitude and k is the wave number of ripplons, respectively, and α is the complex frequency, defined as

$$\alpha = -i\omega_0 - \Gamma \tag{2}$$

Here ω_0 is the angular frequency and Γ is the temporal damping constant. The relation between k and α (dispersion relation) is derived by solving the Navier–Stokes equation [9, 10]

$$\omega_0^2 = (\sigma/\rho)\, k^3 \tag{3}$$

$$\Gamma = 2\nu k^2 \tag{4}$$

using the following conditions: (i) the amplitude is much lower than the wavelength, (ii) there is no motion in deep liquid, (iii) only surface tension

acts on the liquid surface as a vertical stress, (iv) there is no shear stress on the liquid surface, and (v) the effect of gravity is neglected because of short wavelength. Therefore, by measuring the angular frequency ω_0 and the temporal damping constant Γ (density ρ is known), we simultaneously obtain the surface tension σ and the kinematic viscosity ν.

2.2. Optical Heterodyne Detection

We have used the optical heterodyne detection technique so that the intensity of the signals can be clearly detected and can be analyzed in the low-frequency field ($\sim$kHz). The optical heterodyne detection technique is a method in which the scattered light and local oscillating light (we call "reference beam") are mixed, and we obtain the information of the scattered light from optical beat signals. The electric field of the scattered light E_{scat} and reference beam E_{ref} are given, respectively, by [11]

$$E_{\text{scat}}(t) = A_{\text{scat}} \exp[i(\Omega_{\text{scat}} t + \phi_{\text{scat}})] \tag{5}$$

$$E_{\text{ref}}(t) = A_{\text{ref}} \exp[i(\Omega_{\text{ref}} t + \phi_{\text{ref}})] \tag{6}$$

Then the intensity of the mixed beam (interfered light) is represented as

$$\begin{aligned} I(t) &= |E_{\text{scat}}(t) + E_{\text{ref}}(t)|^2 \\ &= A_{\text{scat}}^2 + A_{\text{ref}}^2 + 2A_{\text{scat}} A_{\text{ref}} \cos[(\Omega_{\text{scat}} - \Omega_{\text{ref}})\, t + (\phi_{\text{scat}} - \phi_{\text{ref}})] \end{aligned} \tag{7}$$

Here the third term is the heterodyne signal, which oscillates with amplitude $2A_{\text{scat}}A_{\text{ref}}$ and angular frequency $(\Omega_{\text{scat}} - \Omega_{\text{ref}})$. Thus, it is possible to amplify the scattered light, using a reference beam stronger than the scattered light, and the angular frequency of the optical beat signal $(\Omega_{\text{scat}} - \Omega_{\text{ref}})$ is equal to the angular frequency of ripplon, ω_0.

In our experiment, we transform time field signals into frequency field and analyze them after taking certain time averages to reduce noise. Generally, the displacement of ripplons on the surface is described by damped oscillation (Fig. 1b). Using Fourier transform, we obtain the spectrum of the ripplons (Fig. 1c).

$$P(\omega) \propto \frac{\Gamma}{(\omega - \omega_0)^2 + \Gamma^2} \tag{8}$$

Figure 1c shows a spectrum called Lorentzian with peak frequency ω_0, full width at half-maximum 2Γ. Therefore, we can obtain the parameters in Eqs. (3) and (4) except for the wave number k, provided we can detect and analyze the spectrum of the scattered light coming from the liquid surface.

2.3. Selected Wave Number of the Ripplons Using Diffraction Grating

We suppose that the incident beam with the wave vector K_{in} is incident to the liquid surface with the angle of incidence φ, scattered by ripplon with wave vector k, and the ripplon produces scattered light with wave vector K_{scat} and scattered angle θ. We consider the conservation of momentum equation along the x direction and use the approximation ($K_{in} \approx K_{scat}$) [12] because k is much smaller than K_{in}. Then we obtain

$$k = K_{in} |\sin \varphi - \sin(\varphi + \theta)| \tag{9}$$

Therefore, we can obtain the wave number k of the ripplon provided the angle of incidence φ and scattered angle θ are known. Furthermore, our optical system is set up to be a vertically incident beam. Then $\varphi = 0$, and Eq. (9) simplifies to

$$k = K_{in} \sin \theta \qquad (\because 0 \leqslant \theta \leqslant 90°) \tag{10}$$

In the present study, the beam is divided into two beams by a diffraction grating [6, 13]. As the diffracted beam is generated by the diffraction grating, the diffracted angle between zeroth- and first-order diffracted beams, θ_1, is given by

$$\begin{aligned} d \sin \theta_1 &= \lambda_{in} \\ &= \frac{2\pi}{K_{in}} \end{aligned} \tag{11}$$

Figure 2 shows the concept of the optical system. As two lenses are employed and a diffraction grating is placed in the focus of the first lens, the diffracted beams become parallel due to the first lens and are focused by the second lens at the surface. If both lenses have the same focal length ($f_a = f_b$ in Fig. 2), the intersected angle of the zeroth- and first-order diffracted beams θ_2 is equal to diffracted angle θ_1. The reason is as follows. The distance from A_1 to A_2 and from B_1 to B_2 are the same because two beams between L3a and L3b are parallel. If these focal lengths have been measured and it is clarified that f_a and f_b were the same length, we consider that the distance from G to A_1 is equal to the distance from S to B_2. It is needless to say that the angle $\angle GA_1A_2$ and $\angle SB_1B_2$ are vertical, so the triangle GA_1A_2 and SB_1B_2 are congruent. Therefore, we can determine that θ_1 and θ_2 are the same. Moreover, the scattered angle θ is equal to the intersected angle θ_2, because these beams are specularly reflected on the liquid surface ($\theta_1 = \theta_2 = 0$). Equation (11) then becomes

$$K_{in} \sin \theta = \frac{2\pi}{d} \tag{12}$$

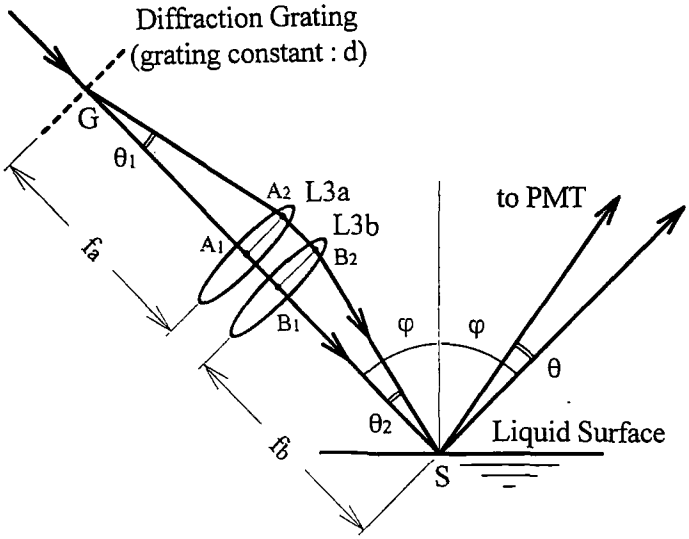

Fig. 2. Schematic diagram showing the diffraction grating and lens system used to select the wave number of the surface wave.

Substitution of Eq. (12) into Eq. (10) finally gives the simple equation

$$k=\frac{2\pi}{d} \tag{13}$$

Previous workers had to measure the incident angle φ and the scattered angle θ when the wave number k is decided; on the other hand, we can easily determine k of the ripplons without measuring φ and θ using Eq. (13), if the focal lengths of the two lenses are equal and the optical system is precisely aligned. But there are two important points for being simple. (i) We must make sure that all focal lengths are exactly equal, and the optical system is precisely aligned ($\theta_1=\theta_2$; diffracted angle θ_1, intersected angle θ_2). (ii) A meniscus must have no effects upon the liquid surface (specular reflection on the surface). If the effect of the meniscus occurs in the surface, it becomes like a concave mirror (or convex mirror), and the scattered angle θ is no longer equal to the intersected angle θ_2.

3. EXPERIMENTAL APPARATUS

Figure 3 shows the present experimental apparatus. A 35-mW He–Ne laser is used for a source of light and is directed to lens L1, a pinhole, and lens L2 to reduce beam extension and to remove spatial noise. Then the

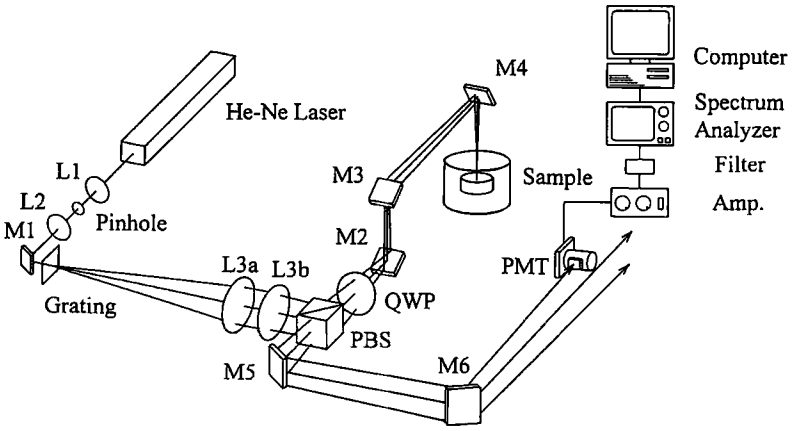

Fig. 3. Schematic diagram of the experimental apparatus.

beam is led to a diffraction grating to be divided into two beams (incident and reference beams), which are necessary for heterodyne detection. These two beams are made parallel by lens L3a and are focused to one point on the liquid surface by lens L3b. Between L3b and the liquid surface, we use a polarized beam splitter (PBS) and a 1/4 wavelength plate (QWP) for vertically polarized incidence. Then the laser light impinging on the liquid surface is scattered around the reflection beam by ripplons. This scattered light with the reference beam is detected by a photomultiplier tube (PMT) using the optical heterodyne technique generated by the diffraction grating. The detected light signals are fitted to a Lorentzian profile with peak angular frequency ω_0 and the full-width at half-maxium 2Γ by the use of the method of least squares. Therefore, in principle, we can obtain the surface tension and the kinematic viscosity using Eqs. (3) and (4). In the present study, we took 128 averages of sampling data in the spectrum analyzer. The $1/e^2$ Gaussian beam radius at the PMT, which is necessary to correct the line-broadening of the spectrum of the ripplons, is measured with a CCD camera and a beam profiler, fitted to a Gaussian, and radaii of x and y axis are determined. All the optical components and sample are fixed to the optical bench to minimize external vibrations.

4. RESULTS

4.1. Measurement of the Focal Length of the Lens

In our experimental apparatus, we select a particular wave number of the ripplons by changing the grating constant. In the case of using

the SLLS method and detecting by optical heterodyne techniques, it is common to determine the wave number by the angle of intersection and incidence. Hence, it is quite difficult to realize the two angles. We eliminate the parameter arising from the angle of incidence, by using vertical incidence. We also determine that the wavelength of the ripplon is equal to the grating constant, although we do not measure the angle of intersection, by setting up the diffraction grating and a sample at the focus of lenses L3a and L3b, respectively. Then the errors in the selected wave number depend only on the grating constant. Accordingly, we measured the focal lengths of lenses L3a and L3b in Fig. 3, accurately. As a result, the focal lengths of L3a and L3b were $f_a = 1184.3$ mm and $f_b = 1183.8$ mm, respectively. This difference had an effect of $<0.1\%$ on the selected wave number. Therefore, we can assume that the wavelength of the ripplons which we observe is equal to the grating constant unless we measure the intersected angle.

4.2. Effect of the Selected Wave Number of the Ripplon

Generally, the intensity of the scattered light of ripplons, I_{scat}, is proportional to the inverse square of the wave number k, [14], i.e.,

$$I_{scat} \propto k^{-2} (\propto \lambda^2) \tag{14}$$

As we mentioned in the previous section, the wavelength of the observed ripplon is equal to the grating constant. Equation (14) shows that the larger the grating constant d, the stronger the intensity of scattered light and, also, the better the S/N ratio is. Then we made an experiment with two diffraction gratings ($d = 100$ and $200\,\mu$m), to verify the differences in the spectrum and the grating constant dependence of surface tension and kinematic viscosity using H_2O at 27°C.

The spectrum of the ripplon at a selected wave number is shown in Fig. 4. Figure 4 indicates that a small wave number k (i.e., large grating constant d) has a better S/N ratio than a large wave number. This indicates that the relation between the intensity of scattered light I_{scat} and the wave number k is in agreement with Eq. (14). The surface tension and kinematic viscosity which are obtained from the spectrum of the ripplons in Fig. 4 are shown in Fig. 5. The dashed lines represent the value in Ref. 15. As for the calculation of the kinematic viscosity, we employed the correction equations given by Hård et al. [16]. Both figures show that the larger grating constant d gives rise to results with small deviations (the average deviation of surface tension is $\sim 0.5\%$, and that of kinematic viscosity is $\sim 10\%$, respectively).

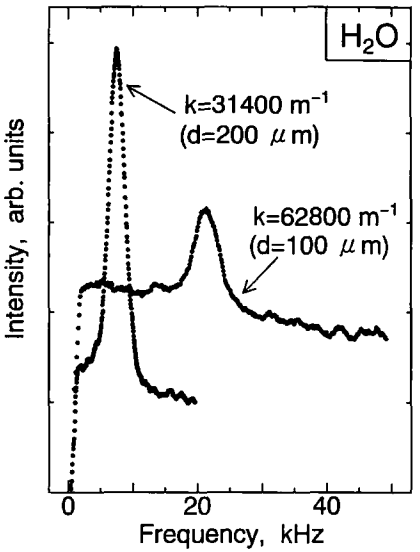

Fig. 4. Differences in the S/N ratio of the spectra for the two gratings. Water, at 27°C.

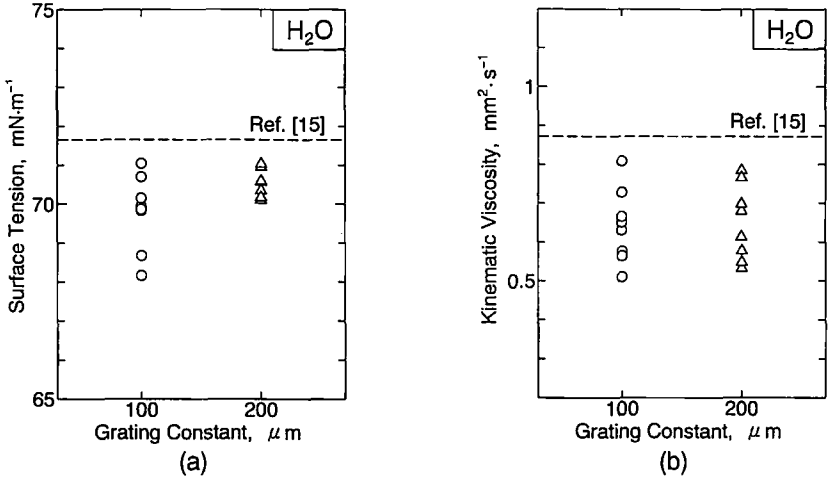

Fig. 5. Grating-constant dependence of the surface tension (a) and kinematic viscosity (b). Water, at 27°C.

Furthermore, as a result of obtaining high S/N ratio waveforms, we could observe the value of surface tension getting smaller as the surface was contaminated. We used a vessel without cleaning and a cover glass so that contamination on the surface was easily promoted and conducted an experiment using water as a sample. Figure 6a shows the time dependence of the spectrum, and Fig. 6b shows the time dependence of the surface tension of water. We had not been able to obtain the decrease in surface tension caused by slight contamination when we used a grating with $d = 100\,\mu m$. However, use of a grating with $d = 200\,\mu m$ caused improvement of the S/N ratio, which made it possible to measure slight differences in the surface tension.

The estimation of accuracy for the measured surface tension and kinematic viscosity is as follows. We estimate that the uncertainty of $\theta_1 = \theta_2$ is 0.05%, that of $\theta_2 = \theta$ is about 0.5%, and that of the grating constant (d) is 0.1%. The uncertainty of the wave number amounts to about 0.65%. The uncertainty of the density is about 0.5%. Therefore, the uncertainty of the surface tension is estimated to be $\pm 2\%$. The kinematic viscosity includes larger experimental errors because we use the correction equation given by Hård et al. [14]. This equation needs as parameters the distance between the water surface and the PMT (R) and the diameter of the interference beam at the PMT (ϕ). We estimate that the uncertainty of R is 0.5% and that of ϕ is 8.5%. R and ϕ are squared, so an uncertainty of 18% is caused by using this equation. Therefore, the uncertainty of the

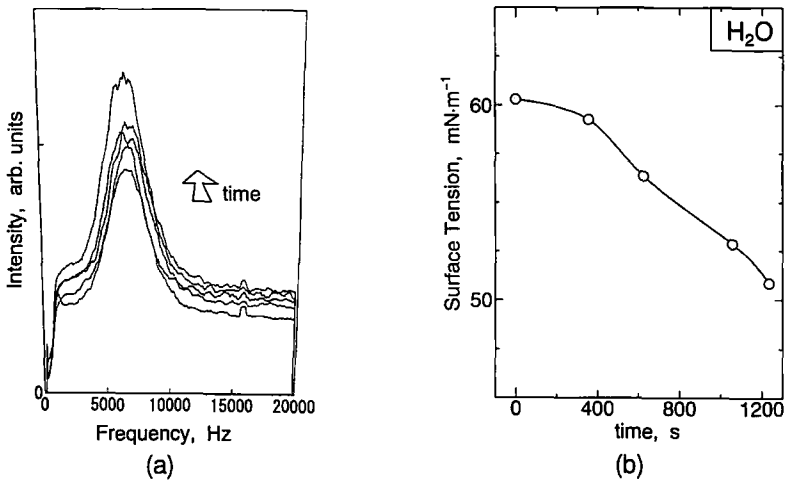

Fig. 6. (a) Time dependence of the spectra caused by contamination of the water surface. (b) Time dependence of the surface tension caused by contamination of the water surface.

kinematic viscosity is estimated to be $\pm 20\%$. We estimate that the uncertainty of the temperature measurement is ± 1 K.

The major direction of our study of the surface laser-light scattering method will be to make the best use of its potential and to apply it to measurements under extreme conditions (such as high-temperature molten Si), which has never been accomplished by conventional methods.

ACKNOWLEDGMENT

The work described in this paper has been supported in part by the Ministry of Education under Grants-in-Aid for Scientific Research (Nos. 05239210 and 04805022).

REFERENCES

1. S. Nakamura and T. Hibiya, *Int. J. Thermophys.* **13**:1061 (1992).
2. Y. Matsuo, Y. Nagasaka, and A. Nagashima, *Proc. 28th Natl. Heat Transfer Symp. Japan* (1991), p. 868.
3. Y. Matsuo and Y. Nagasaka, *Trans. JSME* **B59**(561):185 (1993).
4. R. H. Katyl and U. Ingard, *Phys. Rev. Lett.* **19**(2):64 (1967).
5. R. H. Katyl and U. Ingard, *Phys. Rev. Lett.* **20**(6):248 (1968).
6. S. H. Hård and R. D. Newman, *J. Colloid Interface Sci.* **83**(2):315 (1981).
7. R. B. Dorshow, A. Hajiloo, and R. L. Swofford, *J. Appl. Phys.* **63**(5):1265 (1988).
8. R. B. Dorshow and R. L. Swofford, *J. Appl. Phys.* **65**(10):3756 (1989).
9. H. Lamb, *Hydrodynamics*, 6th ed. (Cambridge University Press, London, 1932), p. 625.
10. V. G. Levich, *Physicochemical Hydrodynamics* (Prentice-Hall, Englewood Cliffs, NJ, 1962), p. 599.
11. E. Wolf, *Progress in Optics, Vol. 8* (North-Holland, Amsterdam, 1970), p. 135.
12. K. U. Ingard, *Fundamentals of Waves and Oscillations* (Cabridge University Press, New York, 1988), p. 478.
13. S. H. Hård and O. Nilsson, *Appl. Opt.* **18**(17):3018 (1979).
14. D. Langevin, J. Jaarinen, and D. Chatenay, *Surfactants in Solution, Vol. 3* (Plenum, New York, 1984), p. 1991.
15. *JSME Data Book: Thermophysical Properties of Fluids* (Japan Society of Mechanical Engineering, Tokyo, 1983), p. 12.
16. S. H. Hård, Y. Hamnerius, and O. Nilsson, *J. Appl. Phys.* **47**(6):2433 (1976).